NACA RM L50H29

NACA

# RESEARCH MEMORANDUM

## POSITIONING INVESTIGATION OF SINGLE SLOTTED FLAPS ON A 47.7° SWEPTBACK WING AT REYNOLDS NUMBERS OF $4.0 \times 10^6$ AND $6.0 \times 10^6$

By Stanley H. Spooner and Ernst F. Mollenberg

Langley Aeronautical Laboratory
Langley Air Force Base, Va.



NATIONAL ADVISORY COMMITTEE
FOR AERONAUTICS

WASHINGTON

October 9, 1950

NATIONAL ADVISORY COMMITTEE FOR AERONAUTICS

RESEARCH MEMORANDUM

# POSITIONING INVESTIGATION OF SINGLE SLOTTED FLAPS ON A 47.7° SWEPTBACK WING AT REYNOLDS NUMBERS OF $4.0 \times 10^6$ AND $6.0 \times 10^6$

By Stanley H. Spooner and Ernst F. Mollenberg

## SUMMARY

A low-speed wind-tunnel investigation has been conducted at Reynolds numbers of $4.0 \times 10^6$ and $6.0 \times 10^6$ to determine the relationship between the flap effectiveness and the horizontal and vertical position of a partial-span single slotted flap on a 47.7° sweptback-wing - fuselage combination. The wing had an aspect ratio of 5.1, a taper ratio of 0.383, and NACA 64-210 airfoil sections.

The value of the maximum lift coefficient is relatively unaffected by the wing-flap position or the flap deflection within the range investigated. The increment of lift coefficient in the linear-lift range, however, varies with flap position and increases with increasing flap deflection. Although the optimum flap position (position of largest lift increment) on a 47.7° sweptback wing is not predicted exactly by two-dimensional tests, the reduction of the increment of wing lift coefficient as a result of the use of the optimum flap positions determined from two-dimensional tests amounts to only 0.02 to 0.03.

## INTRODUCTION

The sensitivity of the maximum lift coefficient to small changes in the position of slotted flaps with relation to the airfoil is shown in reference 1. In the past, two-dimensional tests have been used as the basis for determining the optimum position of these flaps on unswept wings.

With the advent of swept wings there has been some question as to the validity of basing swept-wing flap positions on two-dimensional tests. Furthermore, considerations of the stalling characteristics of some sweptback wings indicate that the wing maximum lift coefficients

may be relatively insensitive to changes in the slotted-flap position so that the optimum flap position must then be established on a basis other than maximum lift.

An investigation was undertaken, therefore, to establish the relationship of the optimum flap positions on a sweptback wing to those determined from two-dimensional tests and to evaluate the effects of flap position. Positioning tests of a partial-span single slotted flap on a $47.7^\circ$ sweptback-wing - fuselage combination were made in the Langley 19-foot pressure tunnel. The wing had an aspect ratio of 5.1, taper ratio of 0.383, and NACA 64-210 airfoil sections normal to the 0.286-chord line. Most of the tests were conducted at a Reynolds number of $4.0 \times 10^6$ and a Mach number of 0.10 and the rest at a Reynolds number of $6.0 \times 10^6$ and a Mach number of 0.14.

## SYMBOLS

The data are referred to a set of axes coinciding with the wind axes and originating in the plane of symmetry at the quarter-chord point of the mean aerodynamic chord. All wing coefficients are based upon the dimensions of the basic wing.

$C_L$ lift coefficient (Lift/qS)

$\Delta C_L$ increment of lift coefficient, measured at $\alpha = 8^\circ$

$\Delta c_l$ increment of section lift coefficient, measured at $\alpha_o = 0^\circ$

$C_D$ drag coefficient (Drag/qS)

$C_m$ pitching-moment coefficient $\left(\frac{\text{Pitching moment}}{qS\bar{c}}\right)$

q free-stream dynamic pressure, pounds per square foot

S wing area, square feet

$\bar{c}$ mean aerodynamic chord, feet $\left(\frac{2}{S}\int_0^{b/2} c^2 dy\right)$

c wing chord parallel to plane of symmetry, feet

c' wing chord measured normal to 0.286c, feet

$b/2$ semispan of wing, normal to plane of symmetry, feet

$y$ spanwise coordinate, normal to plane of symmetry, feet

$L/D$ ratio of lift to drag

$R$ Reynolds number, based on mean aerodynamic chord

$v$ vertical distance of flap reference point to wing reference point (fig. 2), percent c'

$h$ horizontal distance of flap reference point to wing reference point (fig. 2), percent c'

$\delta_f$ flap deflection, degrees

$\alpha$ angle of attack of root chord, degrees

$\alpha_o$ section angle of attack

## MODEL

The principal dimensions of the model are shown in figure 1. Details of the single slotted flaps and the leading-edge flaps are shown in figure 2. A photograph of the model mounted for testing in the Langley 19-foot pressure tunnel is presented as figure 3. The wing, which was of solid-steel construction, had NACA 64-210 airfoil sections normal to the 0.286-chord line. The sweepback of the 0.286-chord line (0.25c') was 45°, the aspect ratio was 5.1, and the taper ratio was 0.383. The wing was uniformly twisted to produce 1.32° washout at the tip and the dihedral angle was 0°. The fuselage was of circular cross section and had a fineness ratio of 10.2.

The round-nose, extensible, leading-edge flaps extended from station 0.500b/2 to 0.975b/2 and had constant chord and constant deflection.

The single slotted flaps had a chord equal to 0.25c' and could be deflected 20°, 30°, or 40°. The flap span was approximately 0.30b/2 and extended from station 0.144b/2 to 0.450b/2. The outboard end of the flap extended only to the 0.450b/2 station since reference 2 indicates that longitudinal stability at maximum lift is unlikely with flaps extending farther outboard. The brackets were so constructed as to permit the flaps to be moved horizontally and vertically in the plane of the given airfoil section in a manner such that the horizontal and vertical positions of the flap reference point were constant

(in percent c') along the flap span. The flap positions were accurate to ±0.001c'. The ordinates for the flap and the flap-well sections are presented in tables I and II.

## TESTS

The tests were conducted in the Langley 19-foot pressure tunnel with the air compressed to approximately 33 pounds per square inch absolute. Most of the tests were made at a Reynolds number of $4.0 \times 10^6$ and a Mach number of 0.10. The Reynolds number of $4.0 \times 10^6$ based on the wing mean aerodynamic chord corresponds to a Reynolds number of $2.9 \times 10^6$ based on the mean chord of the flapped portion of the wing in the plane of the given airfoil section (normal to 0.286c). A few tests were made at a Reynolds number of $6.0 \times 10^6$ and a Mach number of 0.14.

The lift, drag, and pitching moments were measured through an angle-of-attack range at zero yaw by a simultaneously recording balance system. The characteristics of the wing-fuselage combinations were determined for a range of slotted-flap positions and deflections for the model with and without leading-edge flaps. The flap positions investigated are shown in figure 4.

## RESULTS AND DISCUSSION

All data have been reduced to standard nondimensional coefficients and have been corrected for support-tare and interference effects and for air-stream misalinement. Jet-boundary corrections have been applied to the angle of attack and to the drag and pitching-moment coefficients. The jet-boundary induced velocities obtained by means of reference 3 were used to compute these corrections.

Maximum lift.- The lift, drag, and pitching-moment characteristics, representative of the data obtained for the various flap positions, are shown in figures 5 to 8. Within the accuracy of the measurements, the values of maximum lift coefficient are essentially the same over the range of flap positions and deflections investigated, although in two-dimensional tests (reference 1) the maximum lift coefficients obtained were shown to be critically dependent upon the deflection and the relative horizontal and vertical position of the flap with respect to the airfoil. Observations of wool tufts attached to the upper wing surface indicated that the flow separates initially from the outer sections of the wing at moderate angles of attack and spreads inboard along the leading edge. This separation is accompanied by a vortex type of flow as described in reference 4. The tip stall and the complex vortex-flow

phenomena apparently mask the effect of the flaps on the maximum lift coefficient. The increment of lift coefficient $\Delta C_L$, therefore, is used to show the effects of flap position and deflection. It is of interest to note that $\Delta C_L$ is approximately proportional to the change in lift coefficient at which the abrupt decrease occurs in the slope of the lift curve.

Lift increment.- The increments of lift coefficient $\Delta C_L$ measured at $\alpha = 8^\circ$ are presented in the contour plots in figure 9. The increments were determined by using as a base the results of tests with the slotted flaps replaced by a solid trailing edge contoured to the given airfoil section. Although these tests were conducted at a Reynolds number of $6.0 \times 10^6$, reference 4 shows that no scale effect on the lift occurs in the Reynolds number range between $4.0 \times 10^6$ to $6.0 \times 10^6$ so that the use of these results as a base is valid.

Because of the wing sweep and the short flap span, the increments are expectedly small but show a rather orderly variation with a change in flap position. For a flap deflection of $20^\circ$ the increment of lift varies slightly over the range of positions investigated. As the flap-deflection angle is increased up to $40^\circ$, $\Delta C_L$ varies more rapidly with a change in flap position. The position for the maximum value of $\Delta C_L$, however, does not change appreciably with flap deflection. This optimum position of the flap reference point remains about 1 percent ahead of and 2 percent below the wing reference point. The optimum values of $\Delta C_L$ are approximately proportional to the flap deflection and were increasing at the greatest deflection investigated.

The increments of section lift coefficient for deflections of $30^\circ$ and $40^\circ$, obtained from unpublished two-dimensional positioning tests of the same airfoil and flap section at the same Reynolds number ($2.9 \times 10^6$ in plane of given airfoil section) are superimposed on the three-dimensional data presented in figure 9. For the flap deflection of $30^\circ$ the flap position producing the largest lift increment is shown to be nearly the same for either the two- or three-dimensional case. For $\delta_f = 40^\circ$ this optimum position of the flap in two-dimensional flow is displaced upward somewhat from that on the $47.7^\circ$ sweptback wing. The results show that the exact position for maximum $\Delta C_L$ at constant flap deflection produced by a single slotted flap on a $47.7^\circ$ sweptback wing is not predicted by two-dimensional tests but that the reduction of $\Delta C_L$ resulting from the use of optimum flap positions based on two-dimensional tests amounts to a maximum of only 0.02 to 0.03. In addition, the percent change in the lift increment for a given movement of the flap is several times larger for the two-dimensional case than for the three-dimensional case.

Previous tests of the subject wing (reference 2) have shown that some type of leading-edge stall-control device is required on the outer portion of the wing to delay tip stall in the high angle-of-attack range. Flap positioning tests were made, therefore, for the wing equipped with an outboard $0.475b/2$ leading-edge flap.

As shown by the representative data presented in figure 8, the maximum lift coefficients obtained were not appreciably affected by the slotted-flap position. In order to show the effects of flap position, the contours of $\Delta C_L$ obtained from the positioning tests with the leading-edge flaps installed on the wing are presented in figure 10. The region of maximum $\Delta C_L$ is centered approximately about the same point in the contour plot as it is for the configuration without the leading-edge flaps although the area for maximum $\Delta C_L$ is somewhat larger.

The effects of increasing the Reynolds number from $4.0 \times 10^6$ to $6.0 \times 10^6$ are shown in figures 10(a) and 10(b) for the wing configuration without the stall-control device. The effects are similar to those resulting from the addition of the leading-edge flaps in that the area for maximum $\Delta C_L$ is increased, which amounts to a decrease in the sensitivity of the maximum $\Delta C_L$ to flap position.

The flap positions for maximum $\Delta C_L$ for the various configurations investigated are presented in table III.

Drag.- As a means of comparing the drag characteristics, the values of $L/D$ (for an untrimmed lift coefficient of 0.8) measured for the various positions of the single slotted flaps are presented as contour charts in figure 11. A lift coefficient of 0.8 was chosen as representative of that which might be used in the landing-approach condition. The maximum values of $L/D$ at $C_L = 0.8$ are obtained with the flap reference point located ahead of the wing reference point and with the flap almost tangent to the slot lip. Within the range of flap positions investigated the maximum change in $L/D$ with flap position amounted to 0.5.

Two-dimensional positioning investigations of single slotted flaps (reference 5) have shown that the positions for lowest drag generally are incompatible with those for highest maximum lift. A comparison of figures 9 and 11 indicates that the flap positions for maximum $L/D$ (at $C_L = 0.8$) do not differ greatly from those for which the maximum increment in lift is produced. It is realized that the numerous factors involved, such as slot-entry shape, slot-lip shape, and flap-nose shape, influence the characteristics considerably and the trends shown herein are not necessarily representative of designs other than the one investigated.

The effects on the variation of L/D with flap position of the addition of leading-edge flaps and of increasing the Reynolds number from $4.0 \times 10^6$ to $6.0 \times 10^6$ are shown in figure 12 for a flap deflection of $40^\circ$. The addition of the leading-edge flaps results in a reduction in the maximum value of L/D of 0.5 and moved the flap position for maximum L/D rearward. The increase in Reynolds number to $6.0 \times 10^6$ does not greatly alter the flap position for maximum L/D although the value of maximum L/D at $C_L = 0.8$ is increased about 0.4.

The flap positions for the maximum values of L/D at $C_L = 0.8$ for the various configurations investigated are presented in table III.

Pitching moment.- The representative pitching-moment data presented in figures 5 to 8 indicate that the trim variation between the extremes of the flap-position range investigated amounts to a maximum pitching-moment coefficient of about 0.025 for the model with leading-edge flaps and $\delta_f = 40^\circ$. The largest trim change is produced with the flap in the position which gives the greatest lift effectiveness. For flap positions giving equal lift effectiveness the most rearward positions produce the largest negative pitching moments.

The lift, drag, and pitching-moment characteristics of the wing-fuselage combination equipped with the slotted flaps located near their optimum-lift position are presented in figure 13 for a Reynolds number of $6.0 \times 10^6$. Included also are the data for the trailing-edge flaps off with which the lift increments of figures 9 and 10 were determined.

## CONCLUDING REMARKS

From the results of an investigation in the Langley 19-foot pressure tunnel to determine the effects of the position of single slotted flaps on a $47.7^\circ$ sweptback wing, the following remarks may be made:

1. The value of the maximum lift coefficient is relatively unaffected by flap deflection within the range investigated or by position with respect to the wing. The increment of lift coefficient in the linear-lift range, however, varies with flap position and increases with increasing flap deflection.

2. Although the optimum flap position (position of largest lift increment) on a $47.7^\circ$ sweptback wing is not predicted exactly by two-dimensional tests, the reduction of the increment of wing lift coefficient as a result of the use of the optimum flap positions determined from two-dimensional tests amounts to only 0.02 to 0.03.

3. In the range investigated the optimum-lift flap position is little affected by the addition of outboard-located leading-edge flaps or by the increase of Reynolds number from $4.0 \times 10^6$ to $6.0 \times 10^6$.

4. The flap positions at constant flap deflections having the least drag are approximately the same as those for the largest lift increment.

Langley Aeronautical Laboratory
National Advisory Committee for Aeronautics
Langley Air Force Base, Va.

## REFERENCES

1. Cahill, Jones F.: Summary of Section Data on Trailing-Edge High-Lift Devices. NACA Rep. 938, 1949.

2. Salmi, Reino J.: Effects of Leading-Edge Devices and Trailing-Edge Flaps on Longitudinal Characteristics of Two $47.7^{\circ}$ Sweptback Wings of Aspect Ratios 5.1 and 6.0 at a Reynolds Number of $6.0 \times 10^6$. NACA RM L50F20, 1950.

3. Eisenstadt, Bertram J.: Boundary-Induced Upwash for Yawed and Swept-Back Wings in Closed Circular Wind Tunnels. NACA TN 1265, 1947.

4. Salmi, Reino J., and Carros, Robert J.: Longitudinal Characteristics of Two $47.7^{\circ}$ Sweptback Wings with Aspect Ratios of 5.1 and 6.0 at Reynolds Numbers up to $10 \times 10^6$. NACA RM L50A04, 1950.

5. Holtzclaw, Ralph W., and Weisman, Yale: Wind-Tunnel Investigation of the Effects of Slot Shape and Flap Location on the Characteristics of a Low-Drag Airfoil Equipped with a 0.25-Chord Slotted Flap. MR A4L28, 1944.

TABLE I

ORDINATES FOR UPPER SURFACE OF FLAP WELL

[Stations and ordinates given from airfoil chord line in percent airfoil chord.]

| Station | Ordinate (NACA 64-210 airfoil) (a) |
|---|---|
| 74.75 | -0.29 |
| 75.00 | .43 |
| 76.00 | 1.20 |
| 77.00 | 1.60 |
| 78.00 | 1.86 |
| 79.00 | 2.02 |
| 79.75 | 2.11 |
| 84.00 | 1.94 |

[a]Ordinates between stations 79.75 and 84.00 connected by straight lines.

TABLE II

ORDINATES FOR FLAP ON WING HAVING NACA 64-210

AIRFOIL SECTIONS

[Stations and ordinates given from flap-chord line in percent airfoil chord.]

| Upper surface | | Lower surface | |
|---|---|---|---|
| Station | Ordinate | Station | Ordinate |
| 0 | 0 | 0 | 0 |
| .25 | .78 | .25 | -.34 |
| .50 | 1.01 | .50 | -.50 |
| 1.00 | 1.32 | 1.00 | -.70 |
| 2.00 | 1.69 | 2.00 | -.90 |
| 3.00 | 1.89 | 2.50 | -.90 |
| 4.00 | 2.01 | 4.95 | -.70 |
| 5.00 | 2.07 | 9.96 | -.33 |
| 6.00 | 2.09 | 14.98 | -.04 |
| 7.00 | 2.09 | 19.99 | .13 |
| 9.00 | 2.05 | 25.00 | -.05 |
| 11.00 | 1.88 | | |
| 15.04 | 1.30 | | |
| 20.02 | .62 | | |
| 25.00 | .05 | | |

L.E. radius: 0.620
L.E. radius center: 0.170 above flap-chord line

TABLE III

OPTIMUM FLAP POSITIONS

| Leading-edge flaps | $\delta_f$ (deg) | Tests of 0.30b/2 flap on 47.7° sweptback-wing - fuselage combination | | | | | | | | Two-dimensional tests | | |
|---|---|---|---|---|---|---|---|---|---|---|---|---|
| | | Positions for maximum $\Delta C_L$ at $\alpha = 8^\circ$ | | | | Positions for maximum L/D at $C_L = 0.8$ | | | | Positions for maximum $\Delta c_l$ at $\alpha_o = 0^\circ$ | | |
| | | h | v | $\Delta C_L$ | L/D (a) | h | v | L/D | $\Delta C_L$ (a) | h | v | $\Delta c_l$ |
| Off | 20 | 1.50 | 2.00 | 0.208 | 12.8 | 2.00 | 1.25 | 13.0 | 0.200 | ---- | ---- | ----- |
| Off | 30 | 1.25 | 1.80 | .300 | 11.8 | .75 | 1.50 | 12.0 | .295 | 1.00 | 1.50 | 1.450 |
| Off | 40 | .70 | 1.80 | .380 | 10.3 | 1.00 | 1.00 | 10.5 | .355 | 1.00 | 1.00 | 1.740 |
| On | 40 | 0 | 1.00 | .380 | 9.7 | 0 | .50 | 10.0 | .370 | ---- | ---- | ----- |

[a] L/D is measured at $C_L = 0.8$ and $\Delta C_L$ is measured at $\alpha = 8^\circ$ in all cases and both are for $R = 4.0 \times 10^6$.

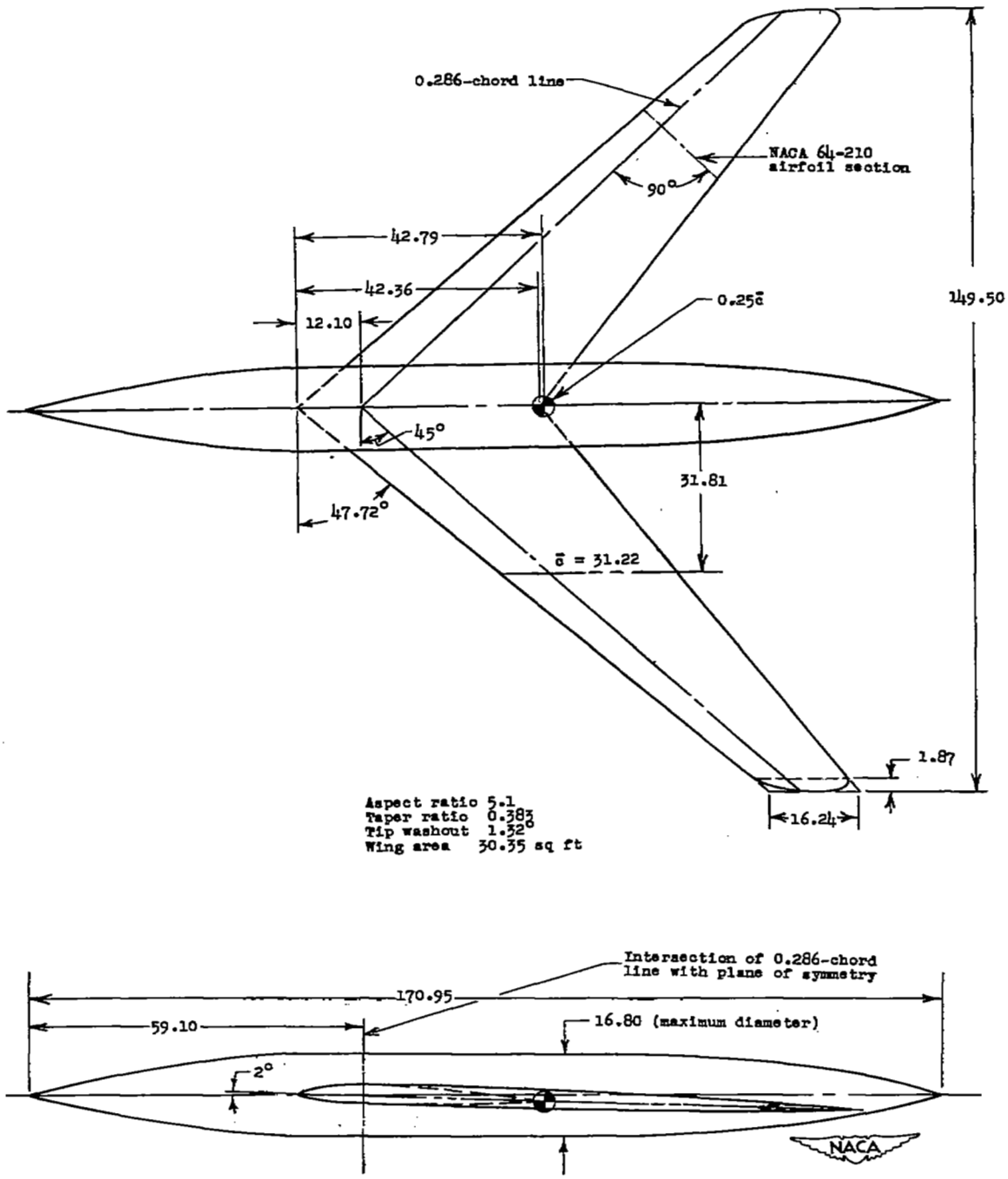


Figure 1.- Geometry of the 47.7° sweptback-wing - fuselage combination. All dimensions are in inches.

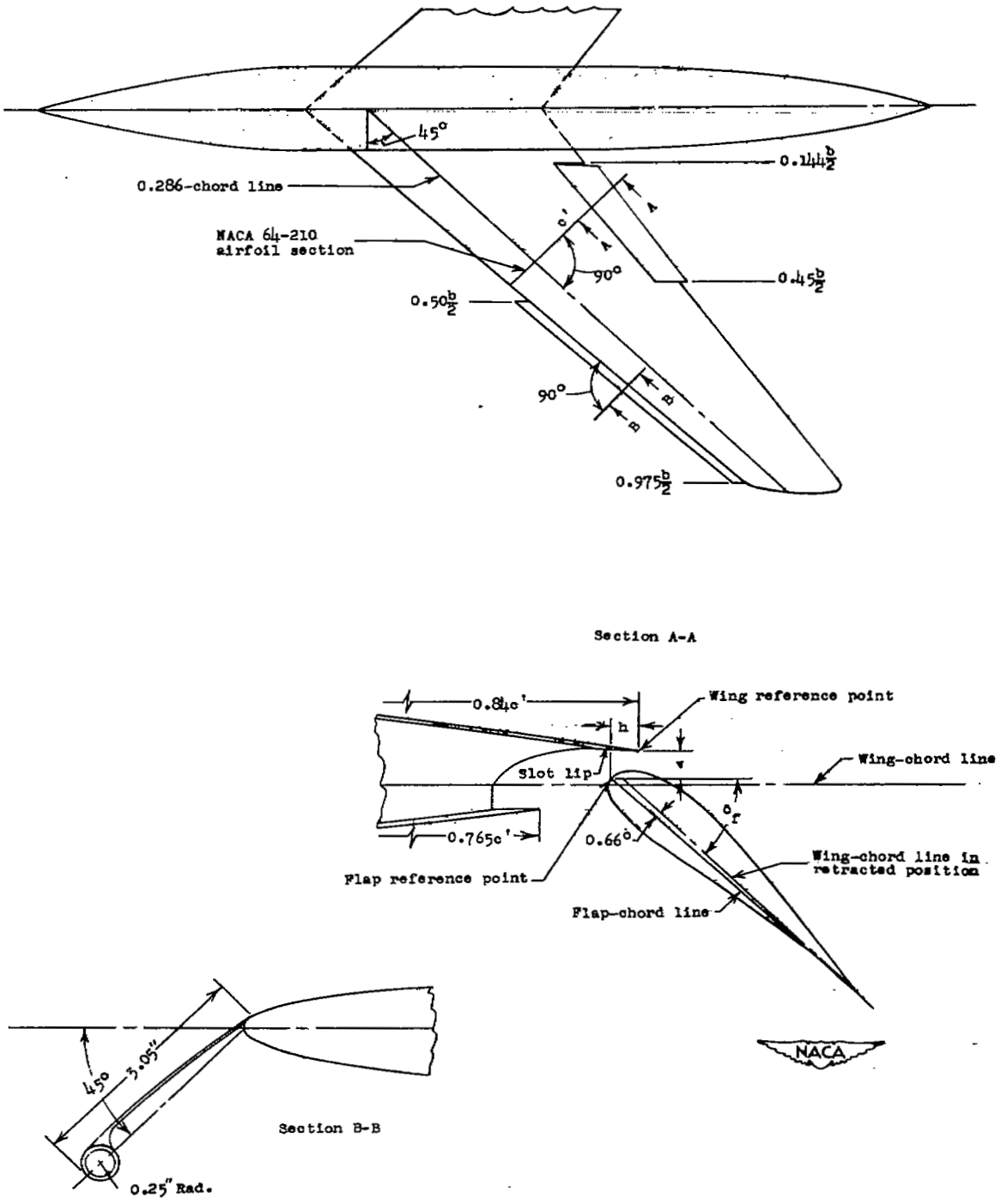


Figure 2.- Details of leading-edge and trailing-edge flaps.

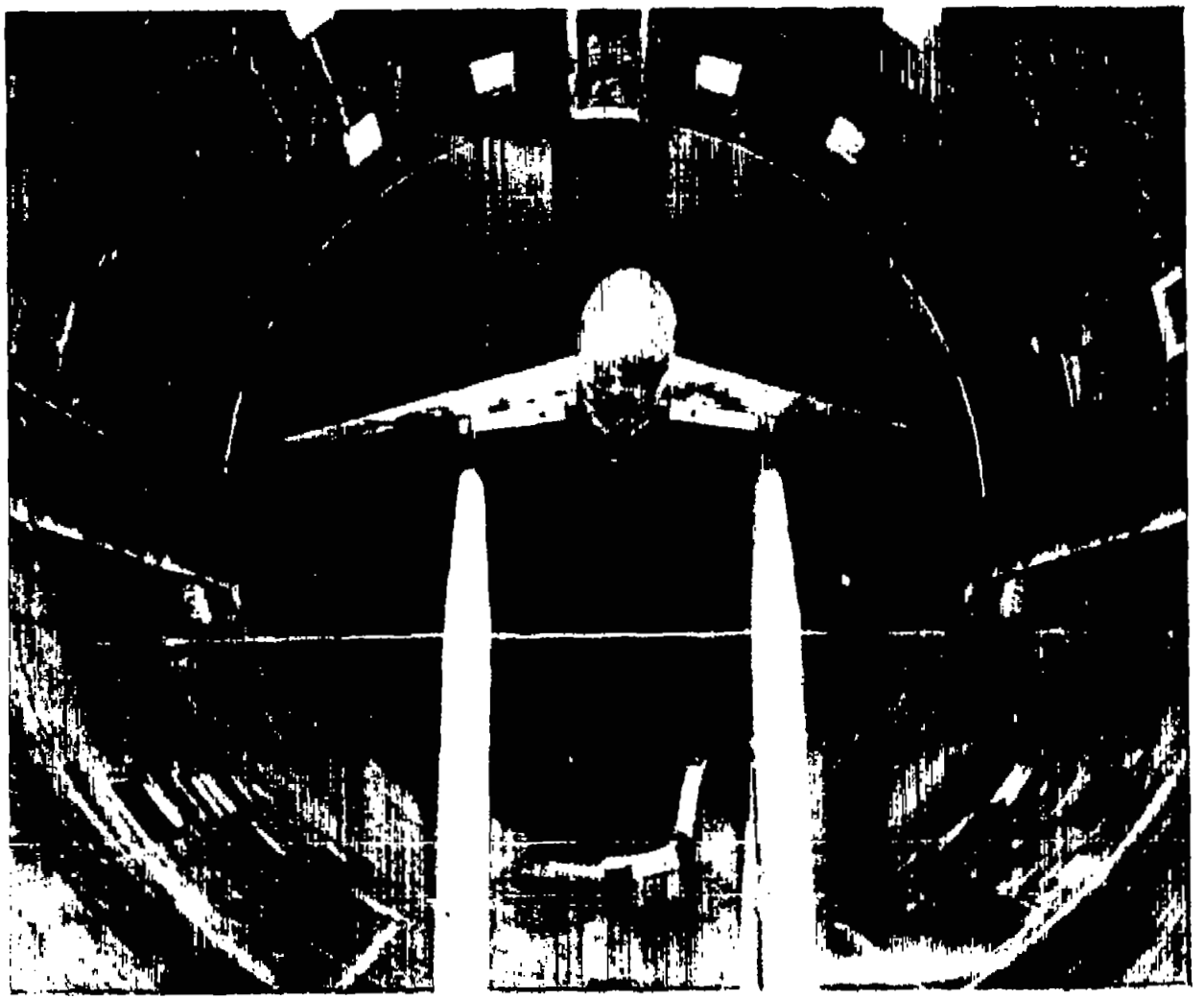

NACA
L-63634

Figure 3.- The 47.7° sweptback-wing - fuselage combination mounted in the Langley 19-foot pressure tunnel.

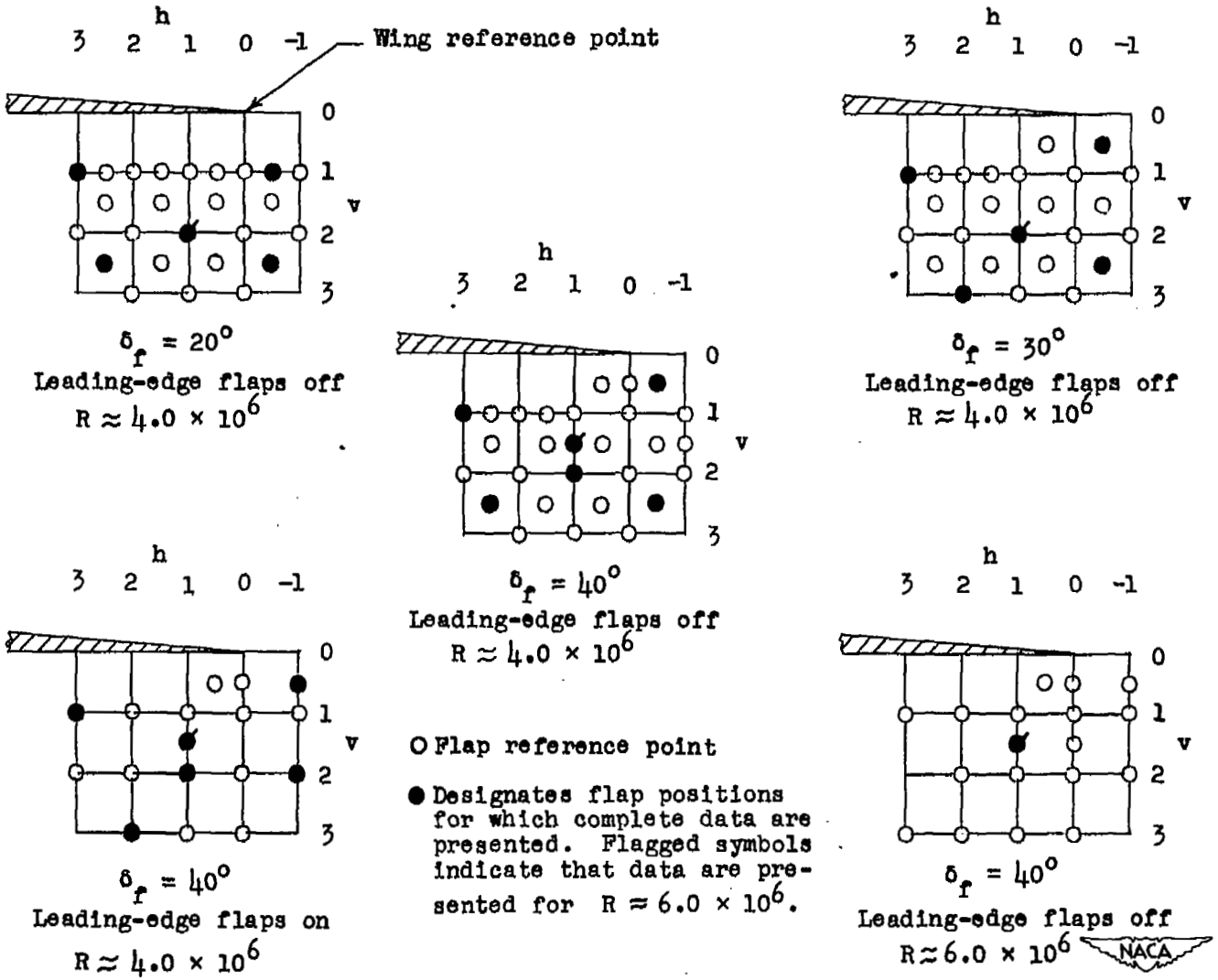


Figure 4.- Index of flap positions investigated.

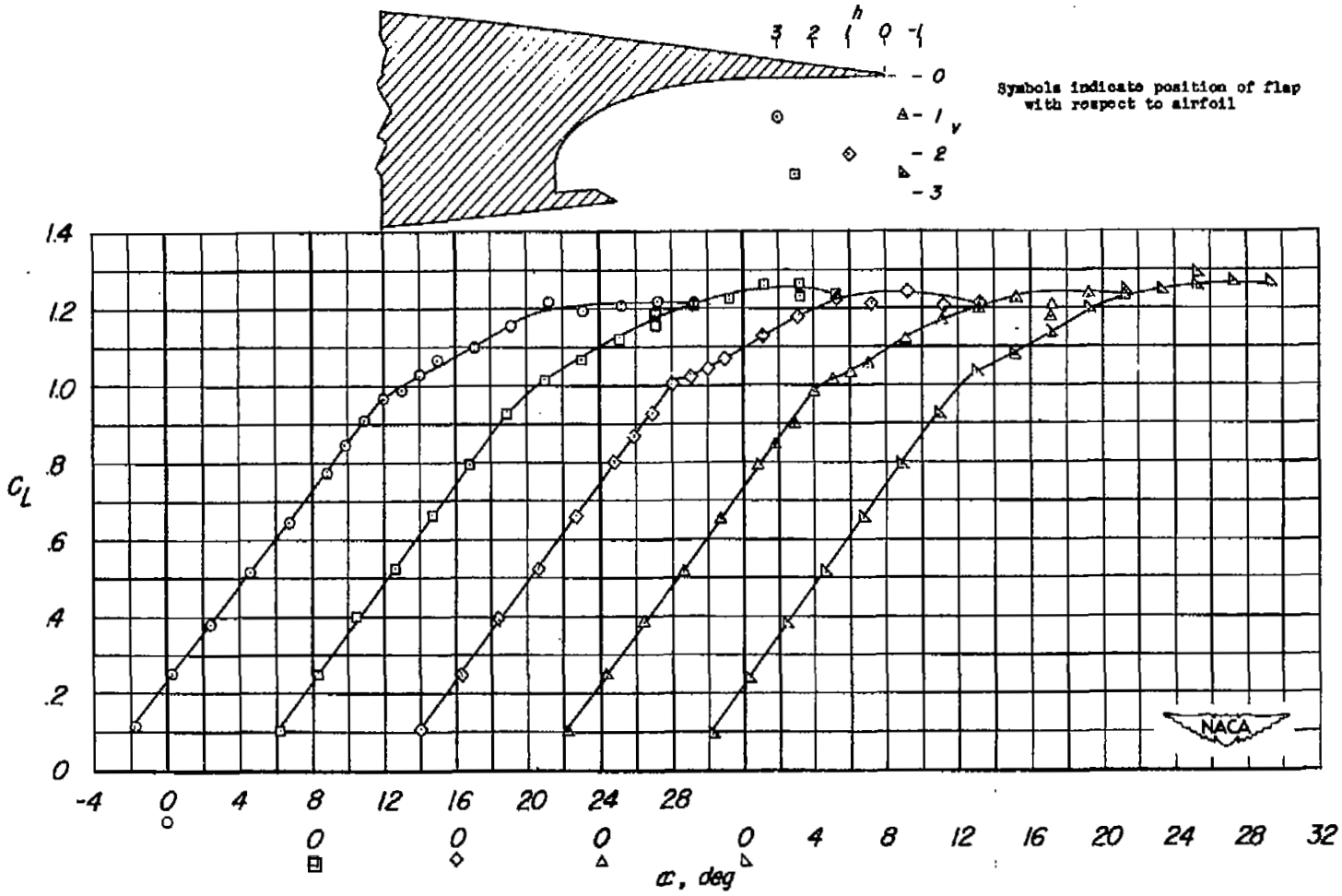


(a) $C_L$ against α.

Figure 5.- Aerodynamic characteristics of wing-fuselage combination for several representative flap positions. Leading-edge flaps off; $\delta_f = 20^\circ$; $R = 4.0 \times 10^6$.

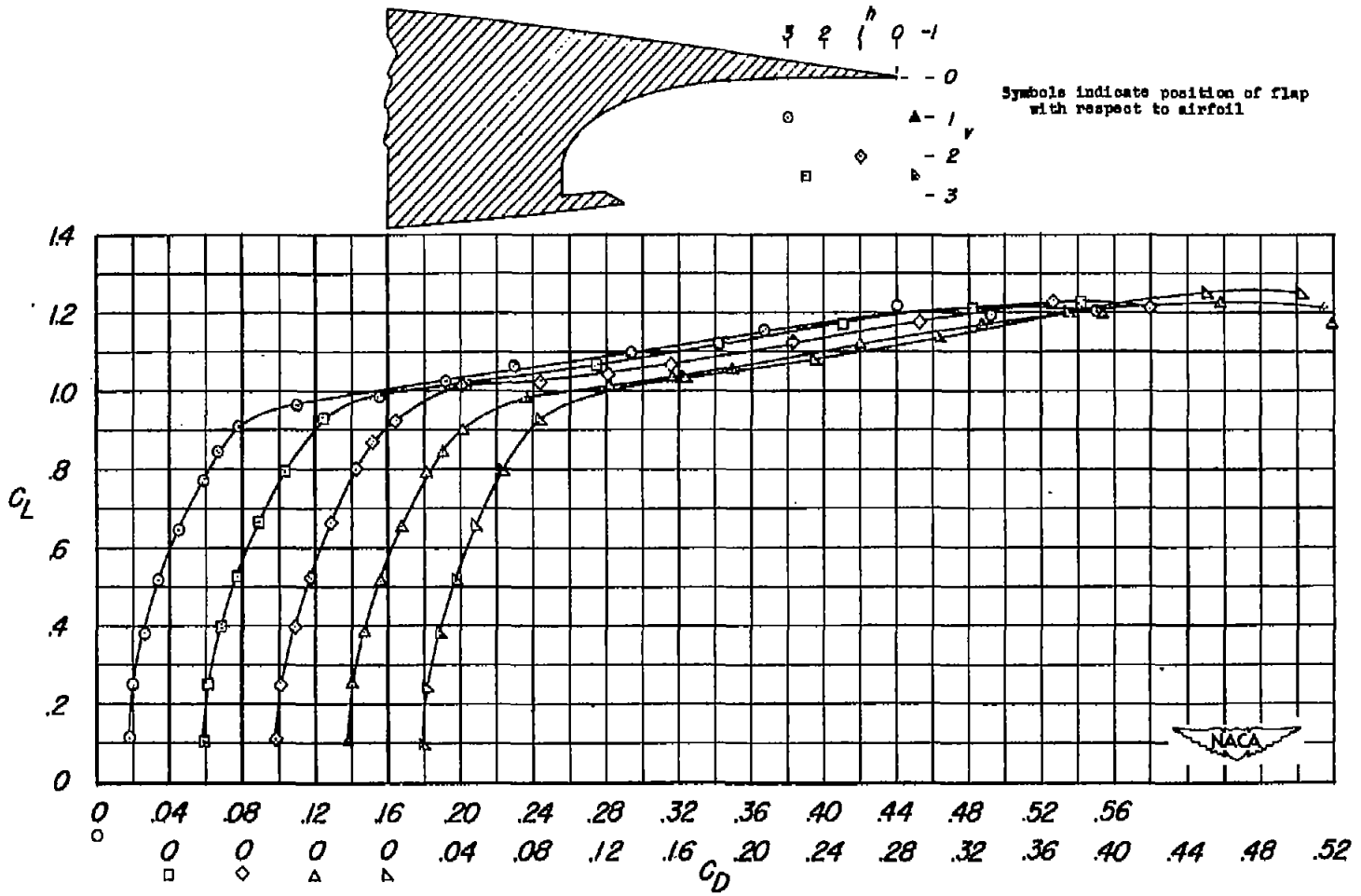


(b) $C_L$ against $C_D$.

Figure 5.- Continued.

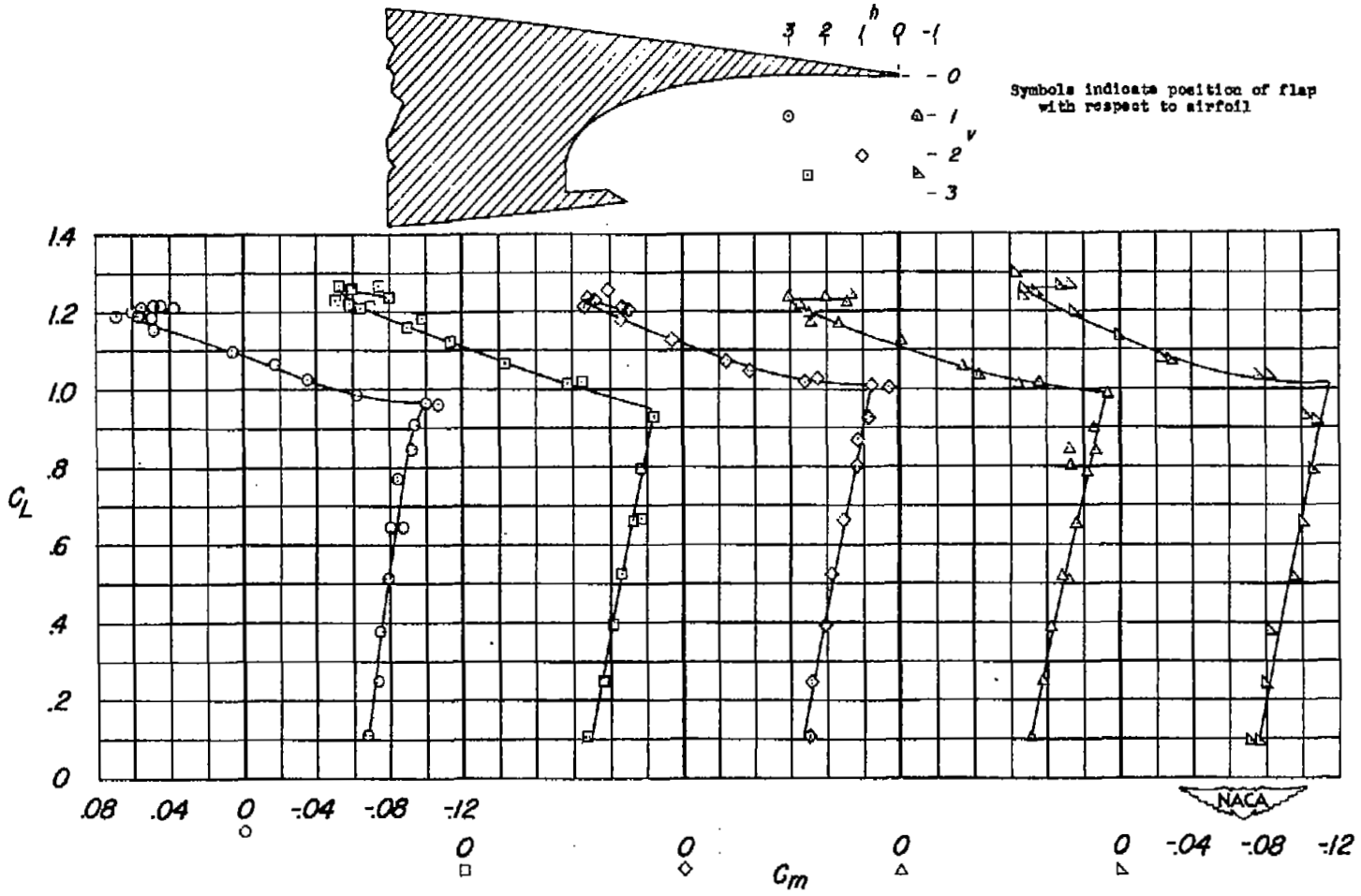


(c) $C_L$ against $C_m$.

Figure 5.- Concluded.

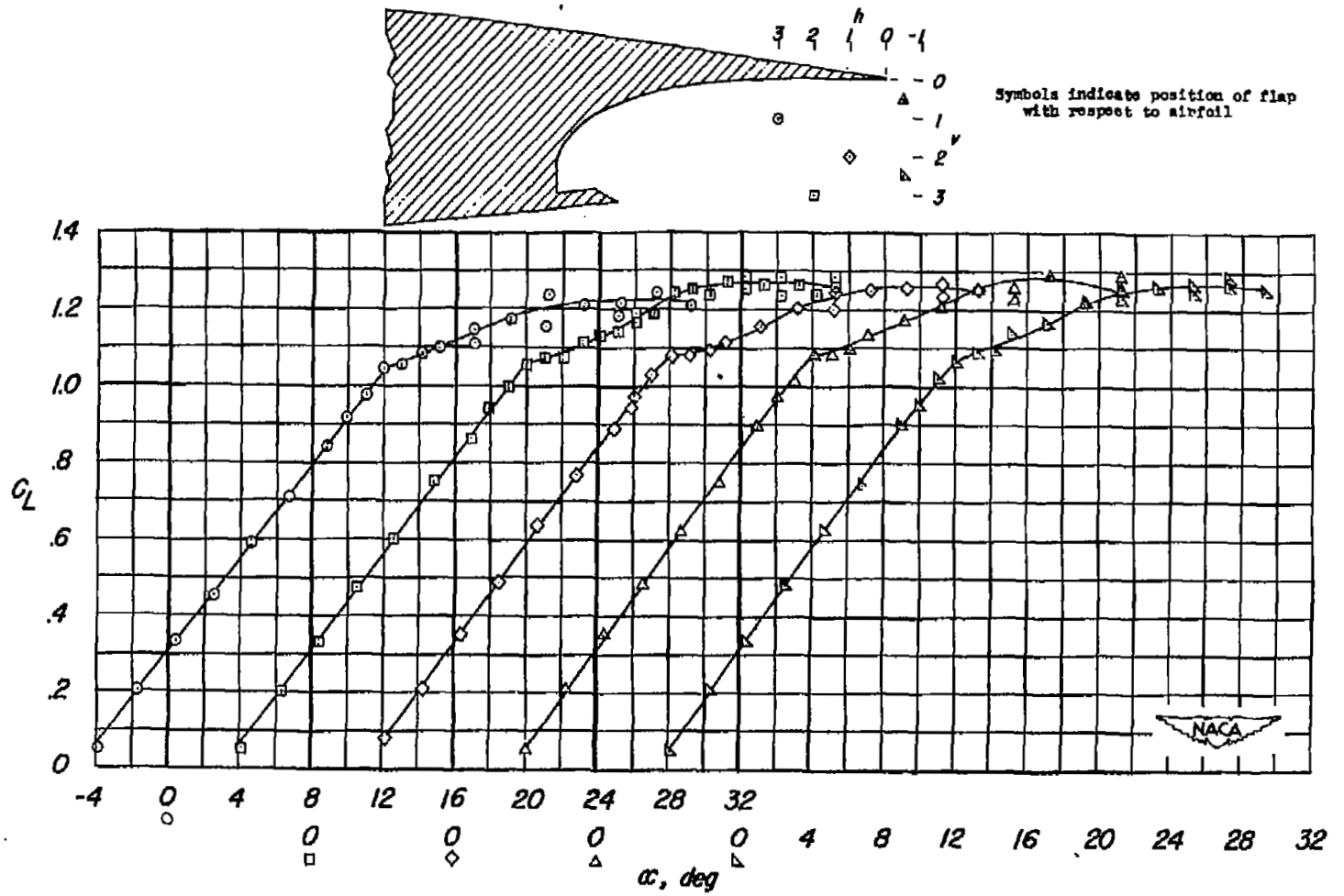


(a) $C_L$ against $\alpha$.

Figure 6.- Aerodynamic characteristics of wing-fuselage combination for several representative flap positions. Leading-edge flaps off; $\delta_f = 30^\circ$; $R = 4.0 \times 10^6$.

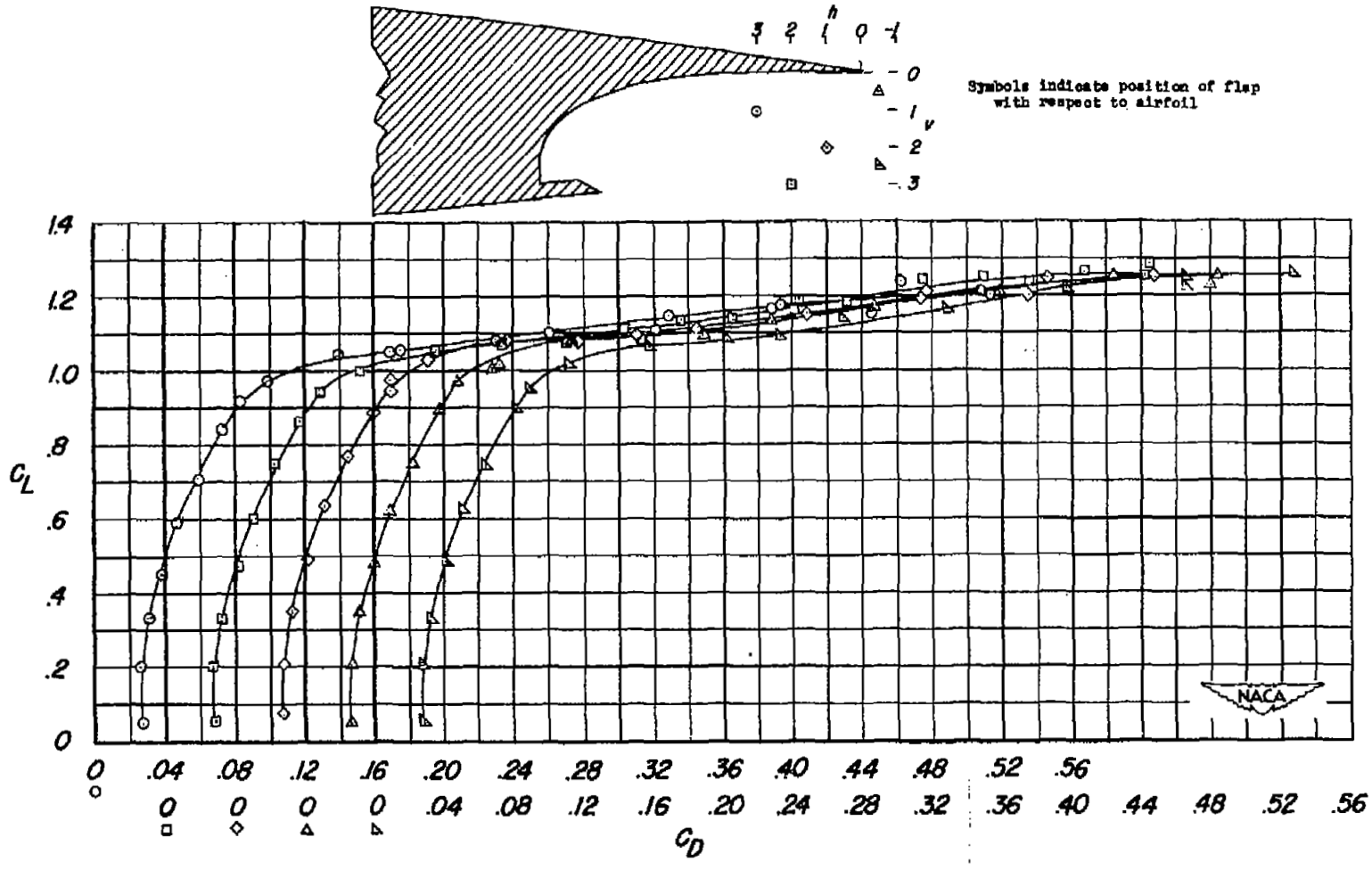


(b) $C_L$ against $C_D$.

Figure 6.- Continued.

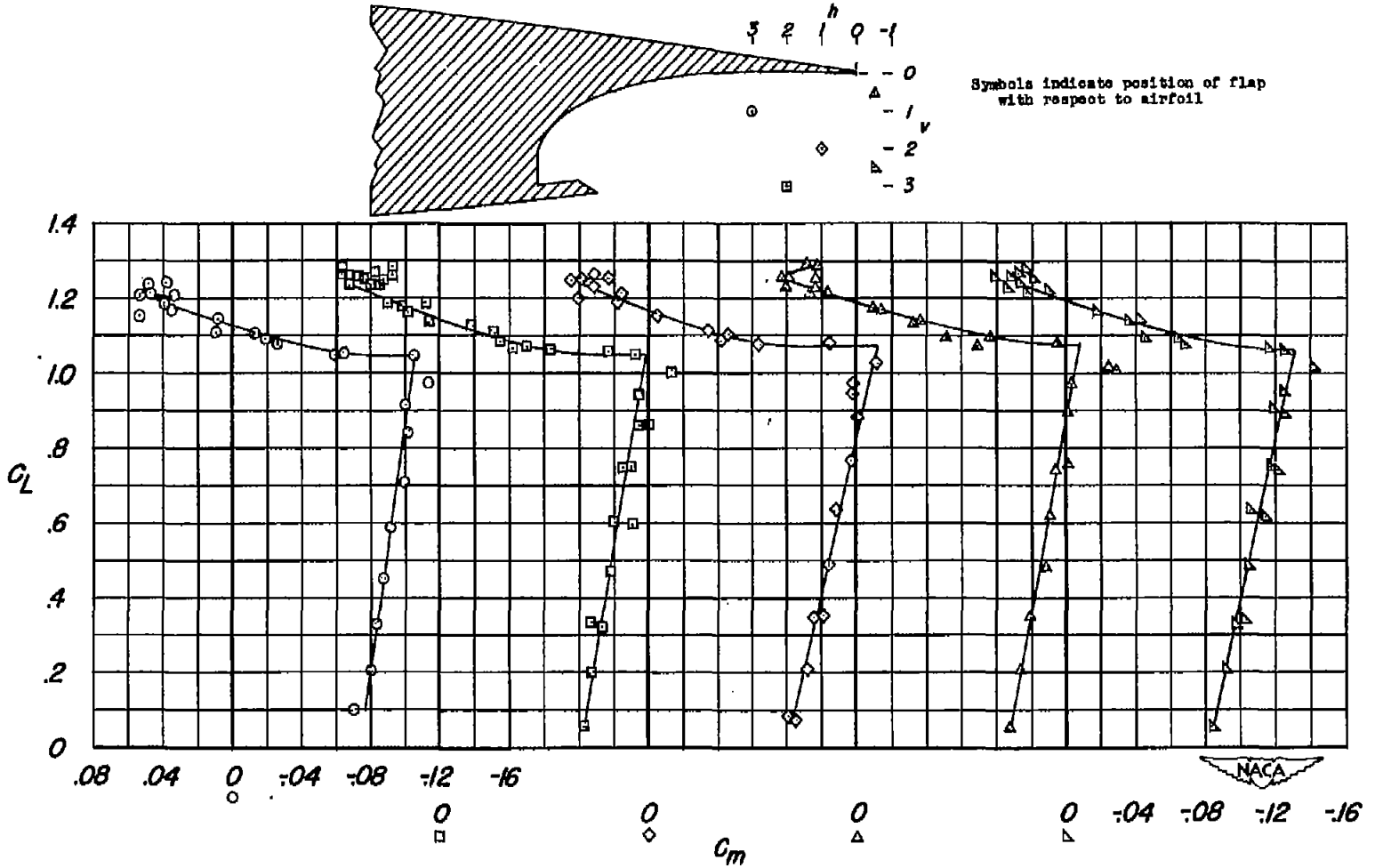


(c) $C_L$ against $C_m$.

Figure 6.- Concluded.

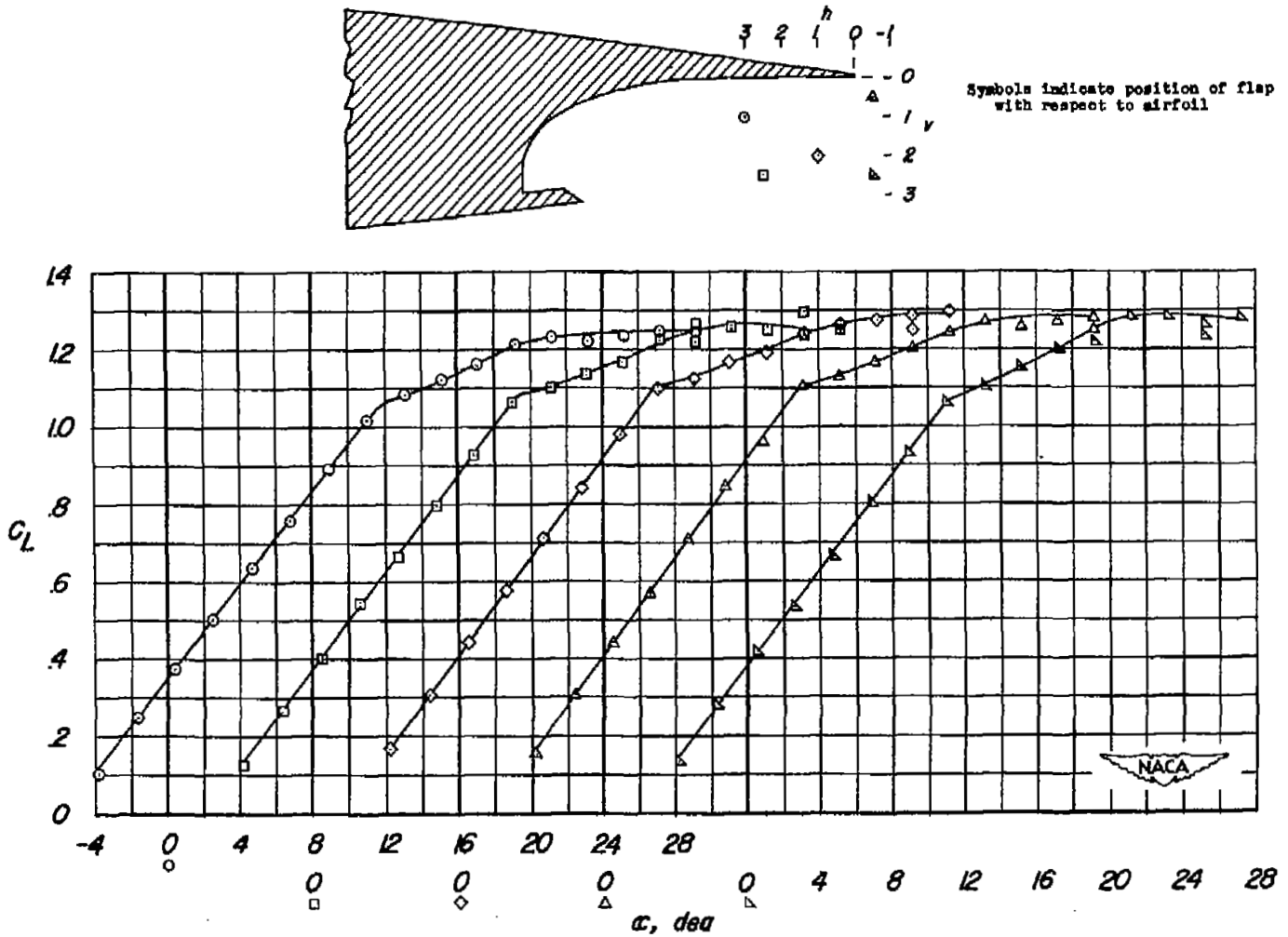


(a) $C_L$ against $\alpha$.

Figure 7.- Aerodynamic characteristics of wing-fuselage combination for several representative flap positions. Leading-edge flaps off; $\delta_f = 40^\circ$; $R = 4.0 \times 10^6$.

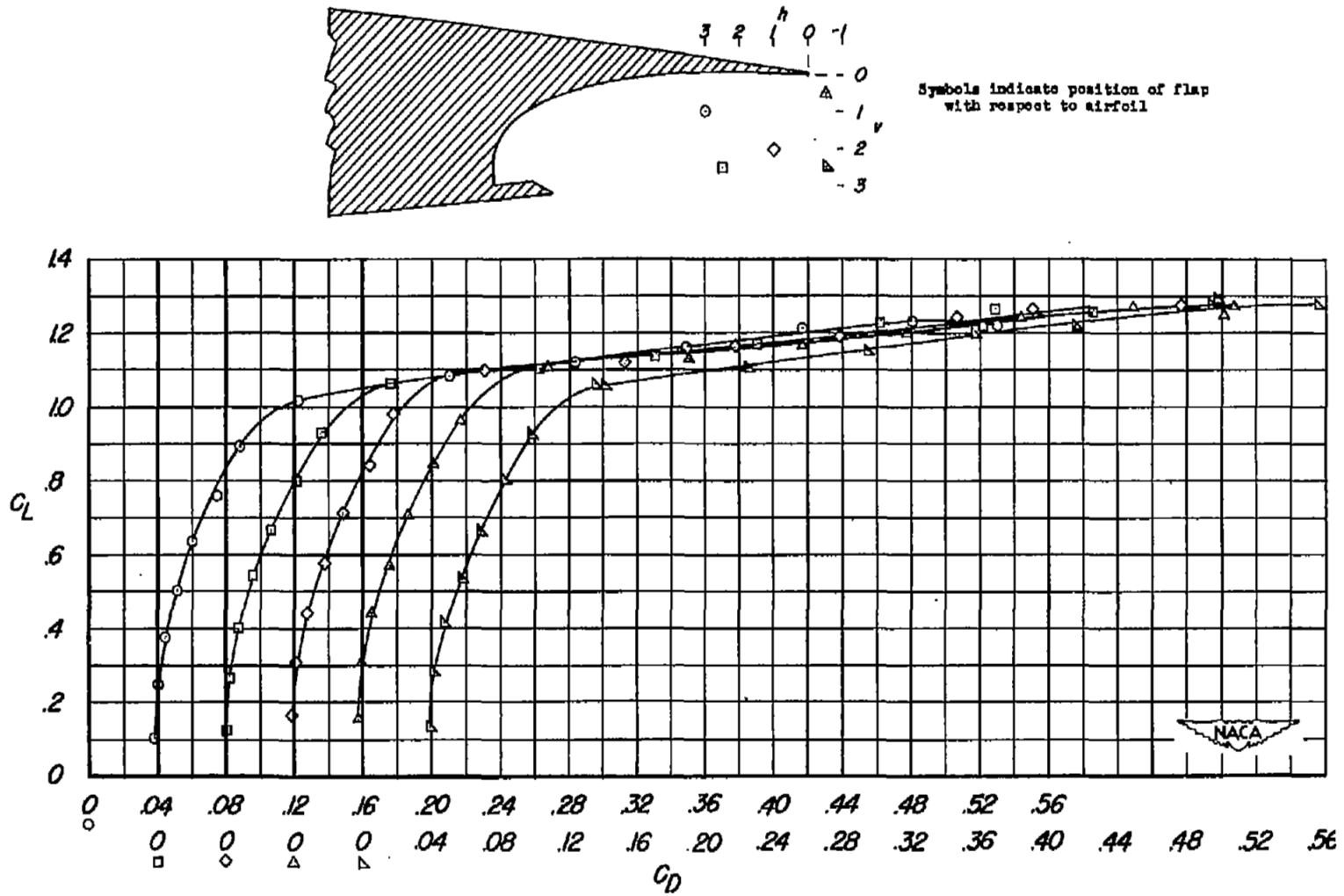


(b) $C_L$ against $C_D$.

Figure 7.- Continued.

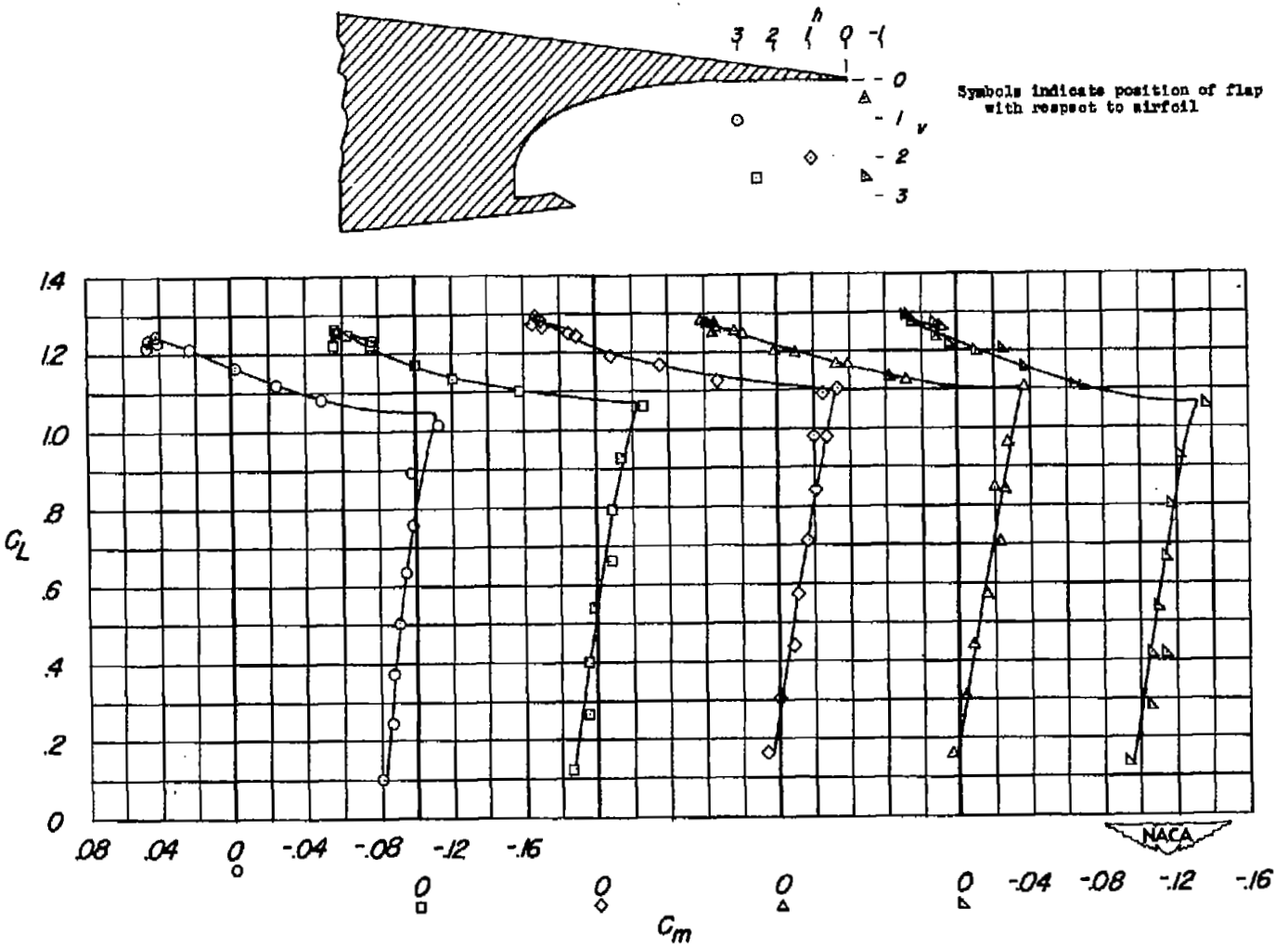


(c) $C_L$ against $C_m$.

Figure 7.- Concluded.

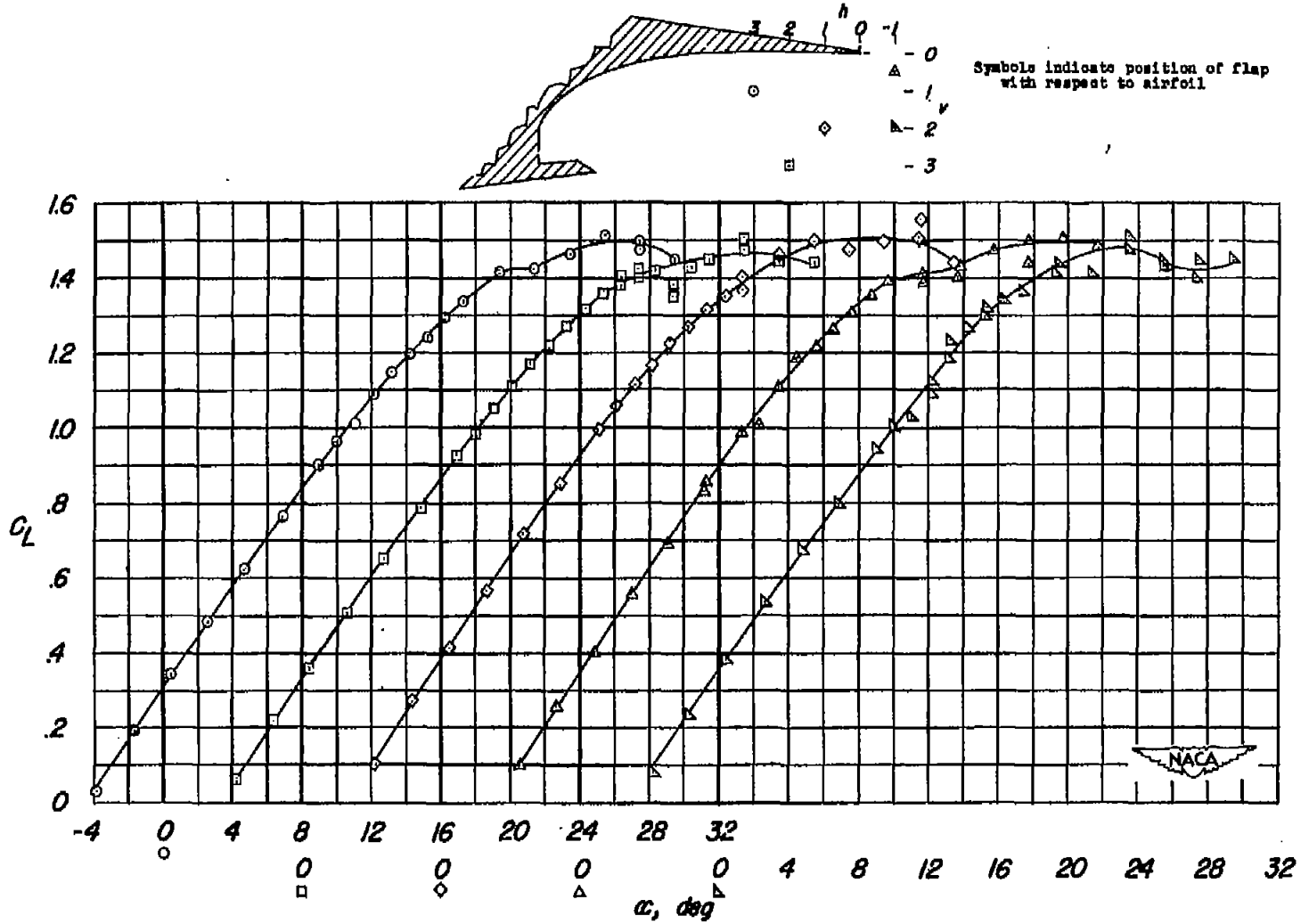


(a) $C_L$ against $\alpha$.

Figure 8.- Aerodynamic characteristics of wing-fuselage combination for several representative flap positions. Leading-edge flaps on; $\delta_f = 40^\circ$; $R = 4.0 \times 10^6$.

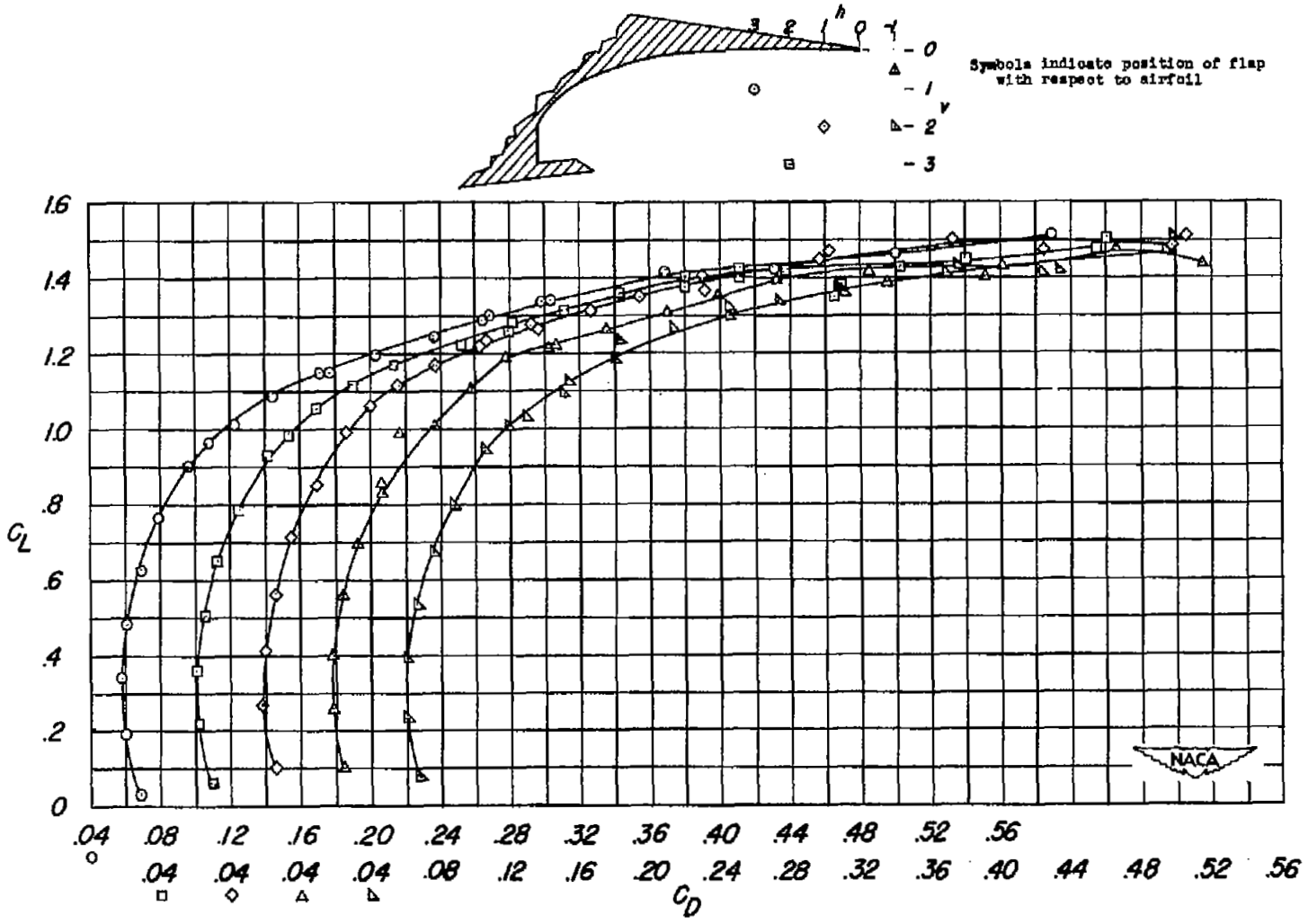


(b) $C_L$ against $C_D$.

Figure 8.- Continued.

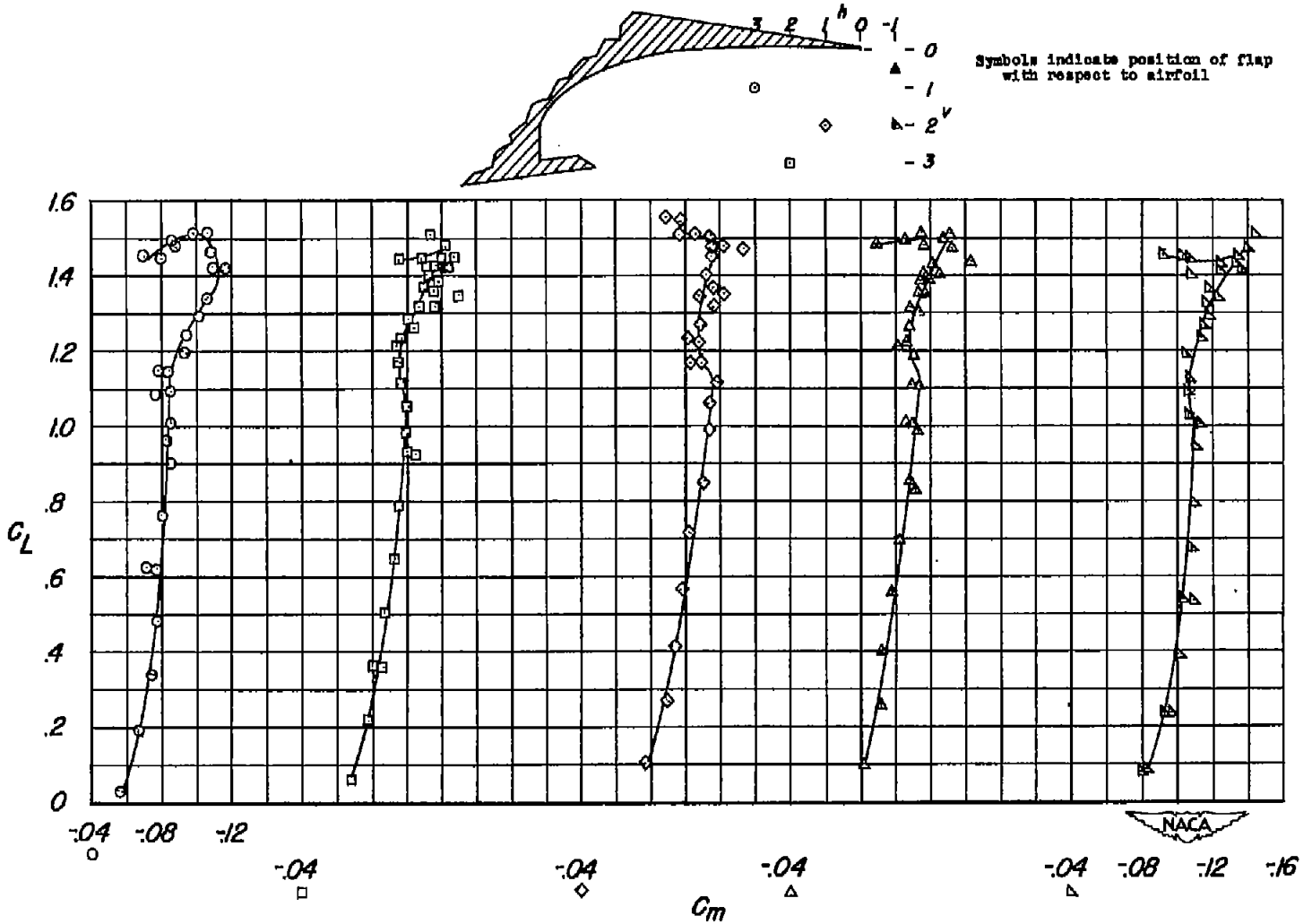


(c) $C_L$ against $C_m$.

Figure 8.- Concluded.

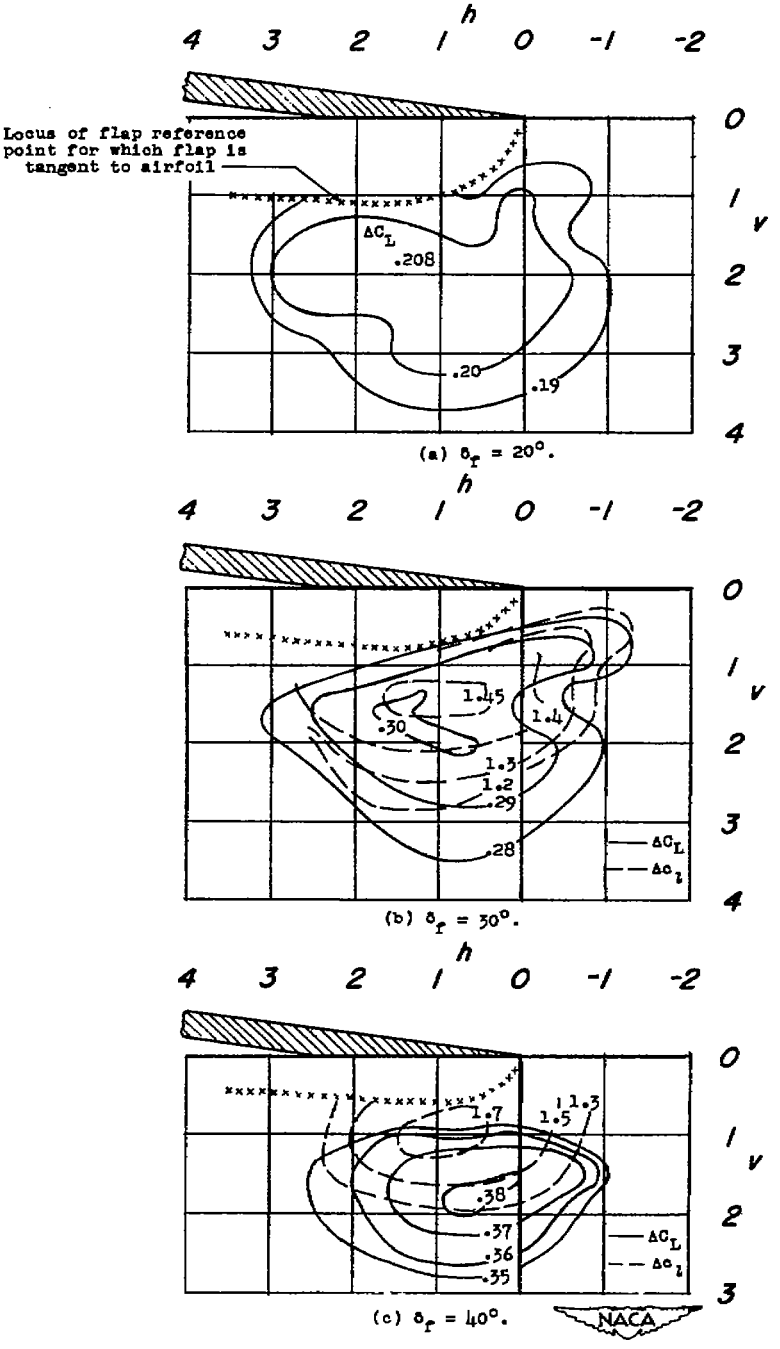


Figure 9.- Increments of wing and section lift coefficient at various positions of the single slotted flaps. Leading-edge flaps off; $R = 4.0 \times 10^6$.

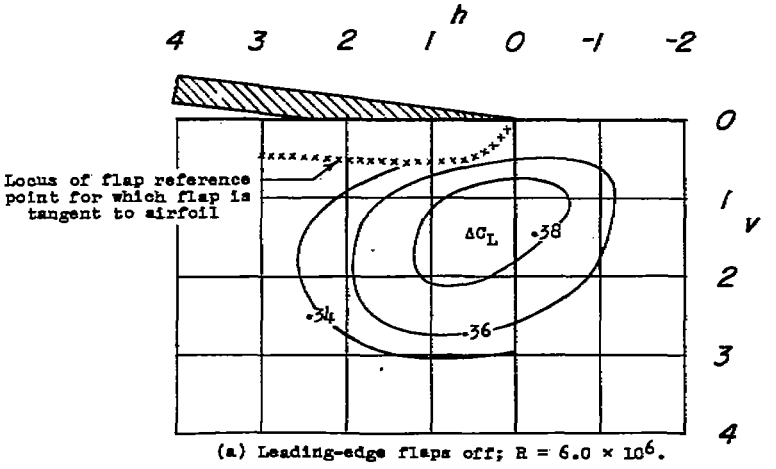


(a) Leading-edge flaps off; R = $6.0 \times 10^6$.

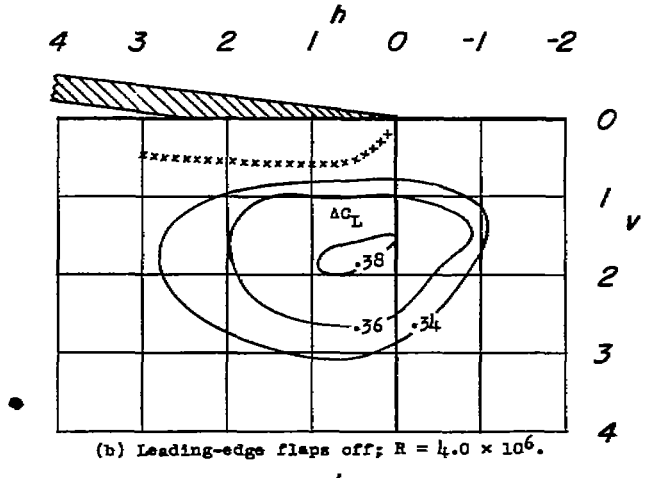


(b) Leading-edge flaps off; R = $4.0 \times 10^6$.

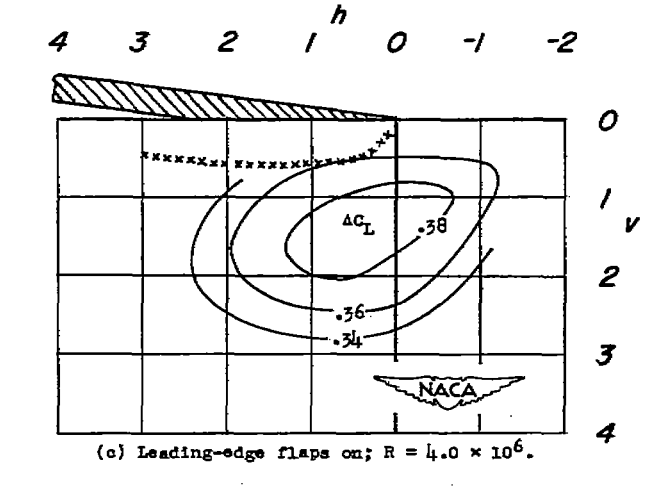


(c) Leading-edge flaps on; R = $4.0 \times 10^6$.

Figure 10.- Increments of wing lift coefficient at various positions of the single slotted flaps. $\delta_f = 40^\circ$.

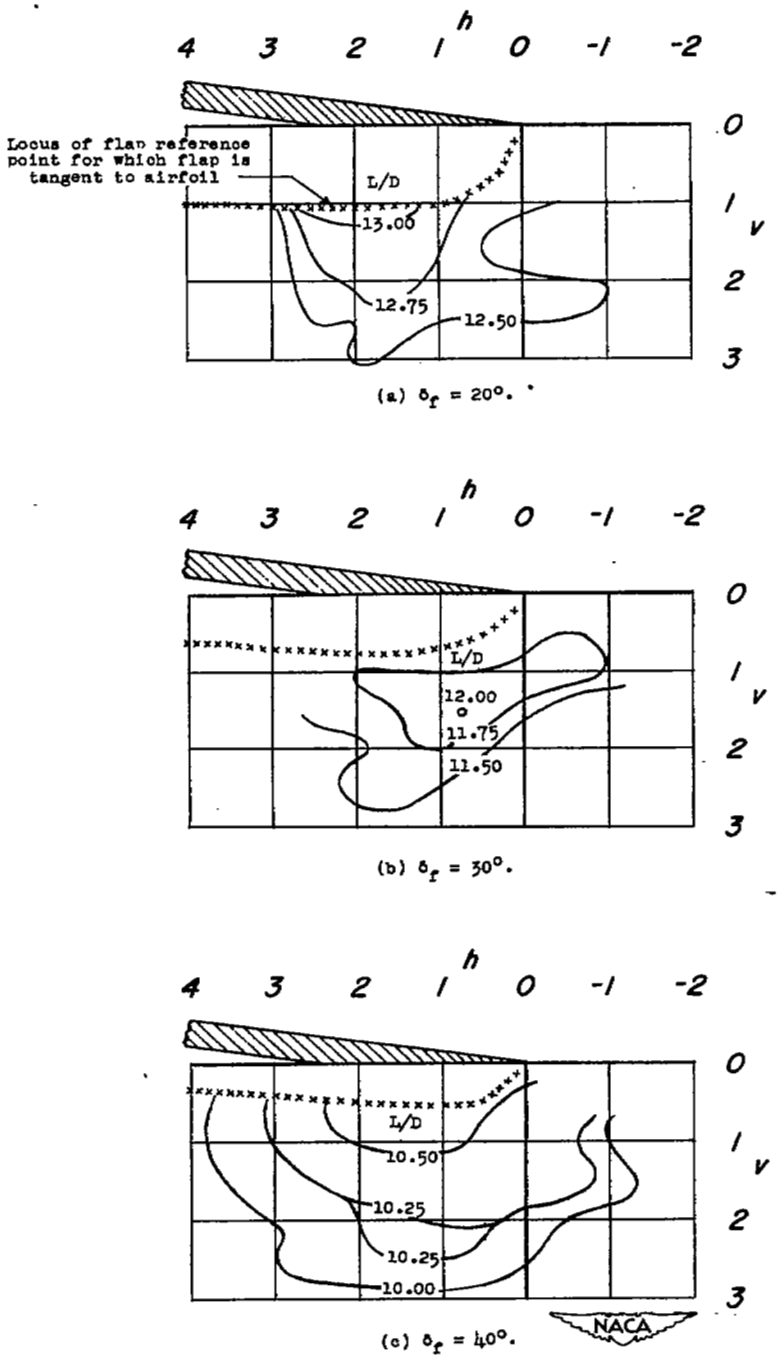


Figure 11.- Values of L/D at $C_L = 0.8$ for various positions of the single slotted flaps. Leading-edge flaps off; $R = 4.0 \times 10^6$.

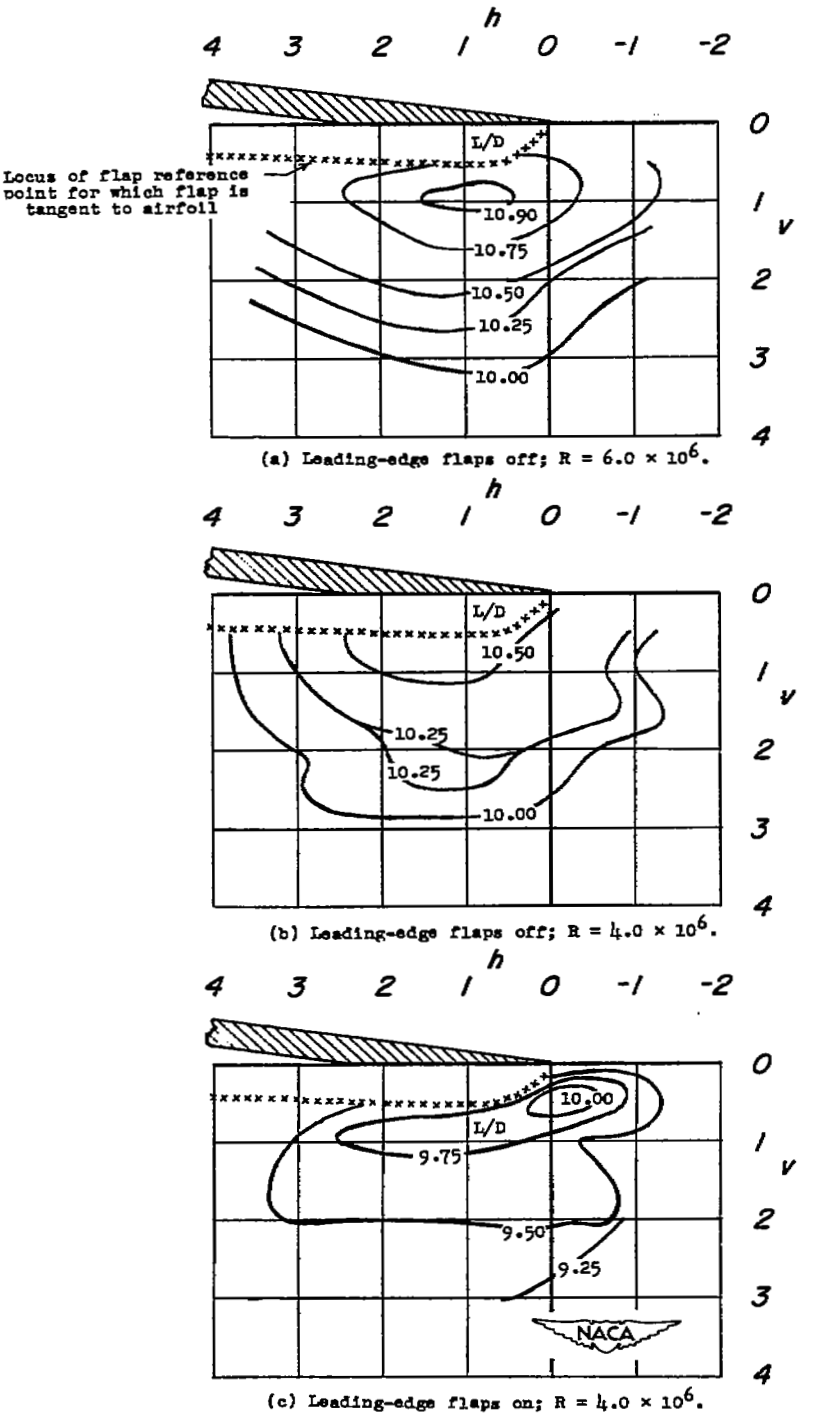


Figure 12.- Values of L/D at $C_L = 0.8$ for various positions of the single slotted flaps. $\delta_f = 40^\circ$.

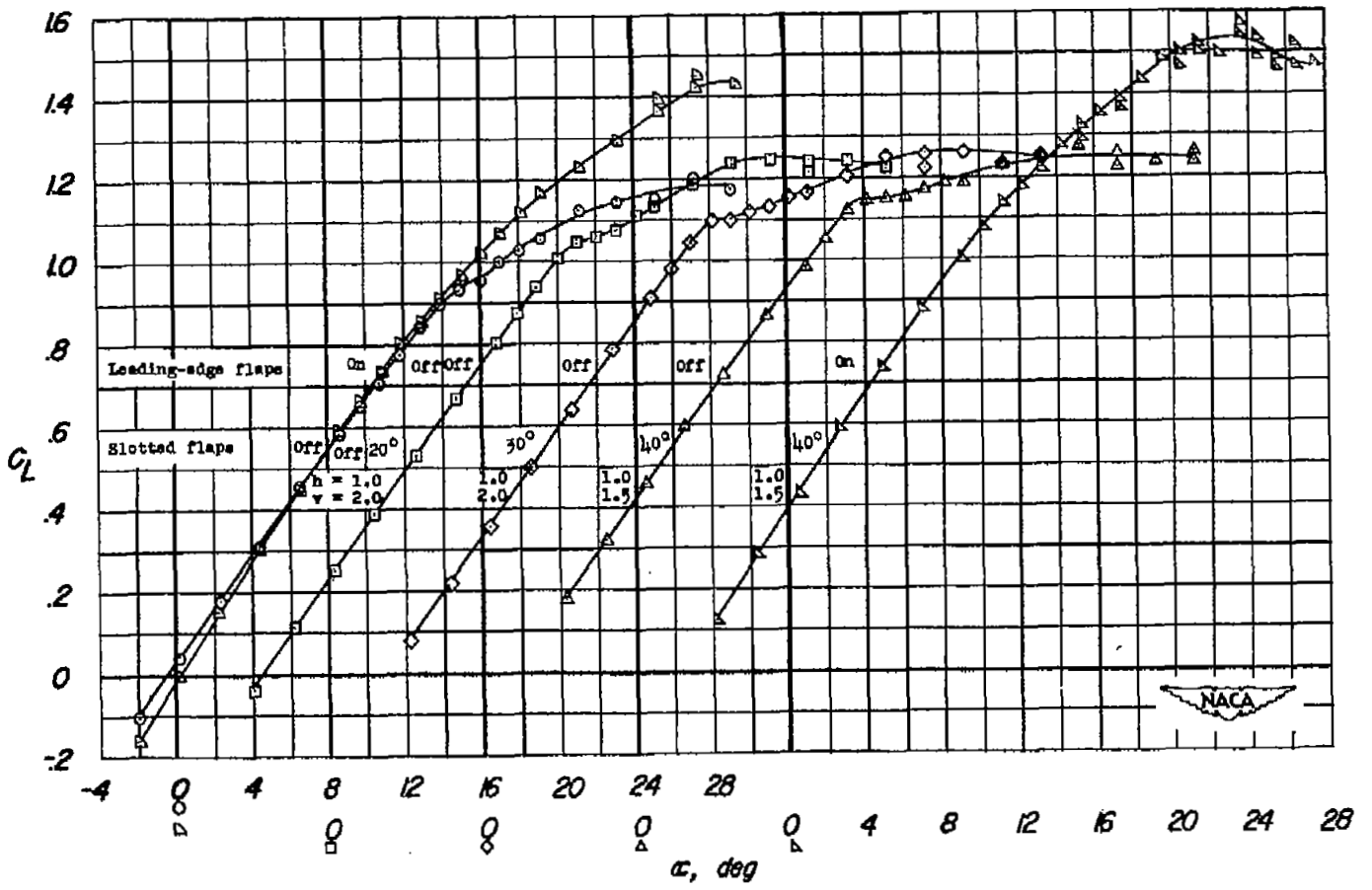


(a) $C_L$ against $\alpha$.

Figure 13.- Aerodynamic characteristics of wing-fuselage combination with single slotted flaps located near the optimum lift position. $R = 6.0 \times 10^6$.

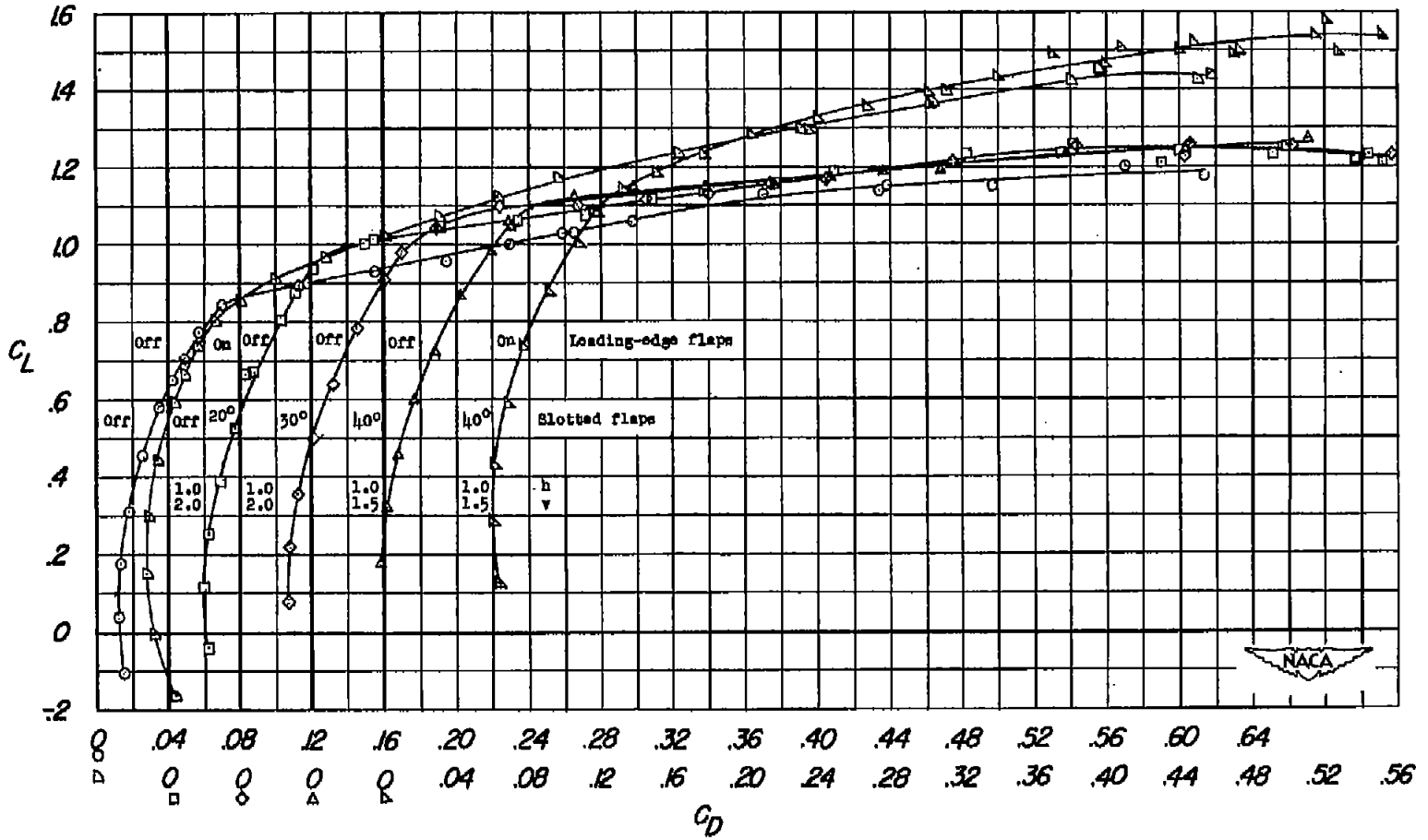


(b) $C_L$ against $C_D$.

Figure 13.- Continued.

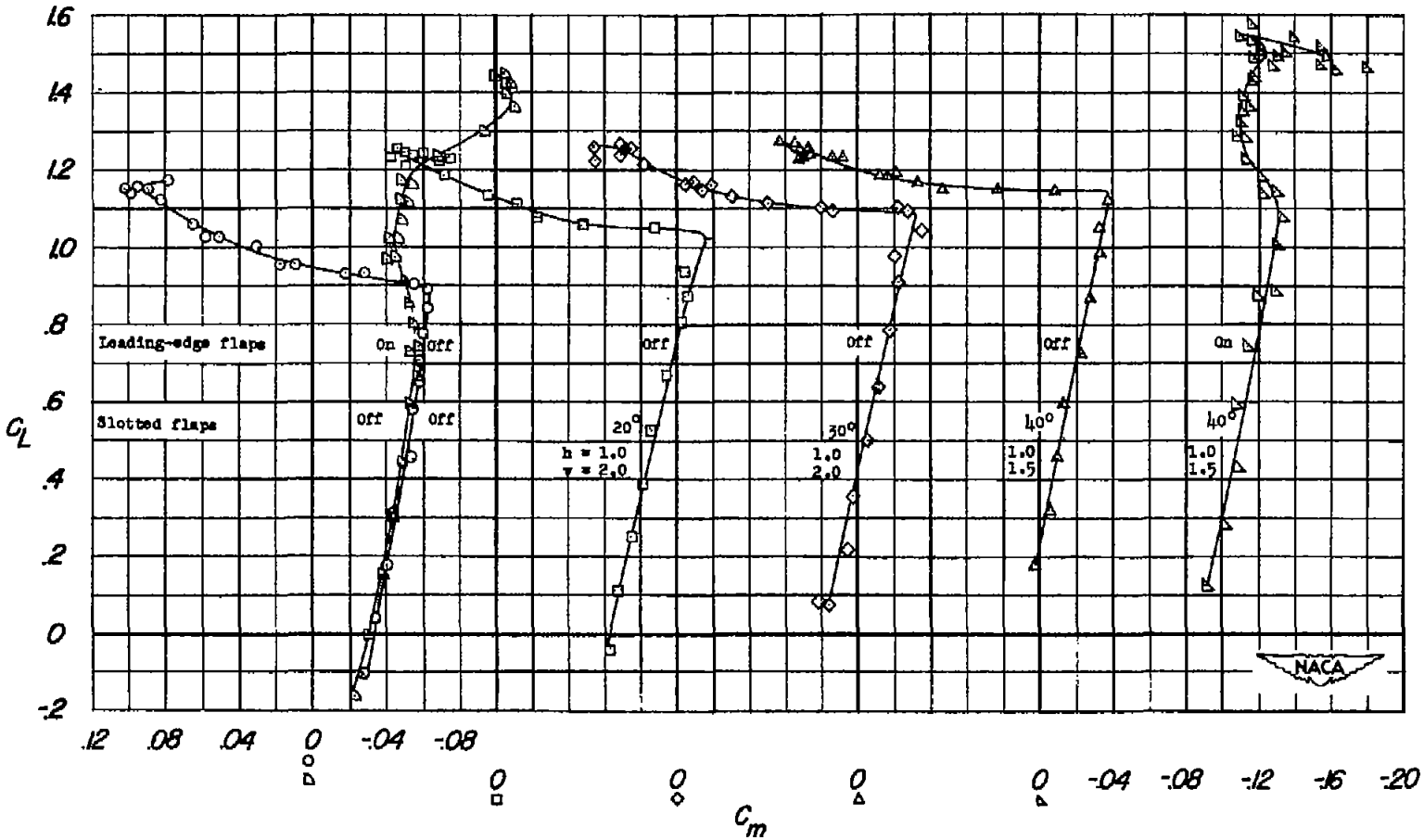


(c) $C_L$ against $C_m$.

Figure 13.- Concluded.